Propagation of Instrumental Errors to the Sky Temperature Measurement

Raul Monsalve

SESE, Arizona State University

May 2, 2013

Description

This report studies the impact on the sky temperature T_{sky}, of deviations in different instrumental parameters from their nominal values.

An idealized instrumental model is assumed, described by equation 13 of the Rogers & Bowman (2012)[1] paper.

The analysis is performed in the range 100-199 MHz.

[1] Rogers, A., & Bowman, J., *Absolute calibration of a wideband antenna and spectrometer for accurate sky noise temperature measurements*, Radio Science, Vol 47, RS0K06, 2012.

Equation for the Sky Temperature

From Equation 13 of the paper:

$$
\begin{aligned}
T_{sky} &= \left[\frac{1-|\Gamma_l|^2}{(1-|\Gamma_a|^2)|F|^2}\right] \times \\
&\left[T_{amb} + T_{cal}\frac{(P_{ant}-P_{load})}{(P_{cal}-P_{load})} - T_u\frac{|\Gamma_a|^2|F|^2}{(1-|\Gamma_l|^2)}\right. \\
&\left. -\,(T_c \cos\phi_{aF} + T_s \sin\phi_{aF})\frac{|\Gamma_a||F|}{(1-|\Gamma_l|^2)}\right] \qquad (1)
\end{aligned}
$$

- $F = \frac{\sqrt{1-|\Gamma_l|^2}}{1-\Gamma_a\Gamma_l}$
- $\phi_{aF} = phase(\Gamma_a \cdot F)$

Methods

Errors are expected on the following vector parameter:

$$\bar{\theta} = (T_{amb}, T_{cal}, T_c, T_s, T_u, |\Gamma_a|, \phi_a, |\Gamma_l|, \phi_l) \tag{2}$$

These errors are propagated to the sky temperature using two methods:

1. Calculus-based approach (Taylor expansion, assuming small errors)
2. Perturbation-based approach

Both cases require the use of the nominal value and the error assigned to each of these parameters.

Computations are performed at a frequency resolution of 1 MHz, and in some cases interpolation or model-fitting are necessary to take the data to this resolution.

The following slides present the nominal values of the parameters along with a brief description.

Fiducial Values: Ambient and Excess Temperature

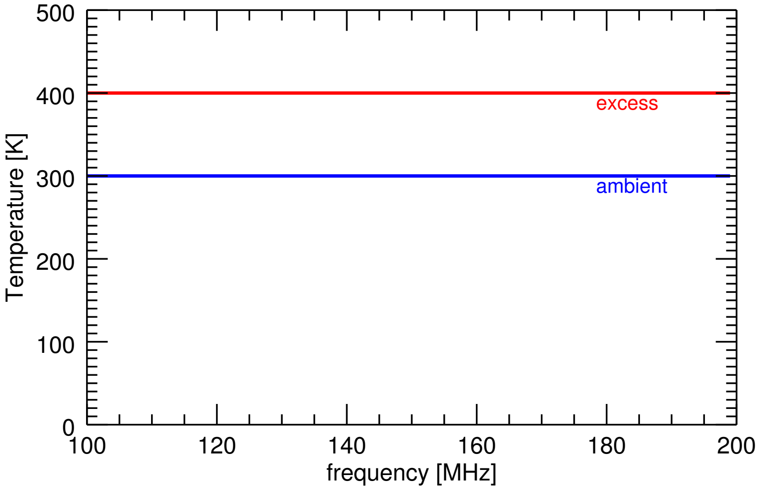

Figure: Nominal values of 300 K and 400 K are used for the ambient and excess temperatures.

Fiducial Values: Noise Wave Parameters

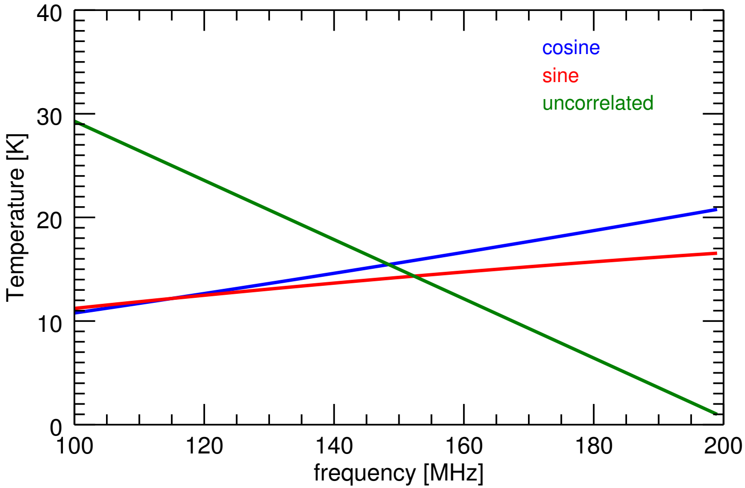

Figure: These values and slopes were obtained from the Rogers & Bowman (2012) paper, figure 8. They were projected to the 100-199 MHz range at 1 MHz resolution.

Fiducial Values: Spectra

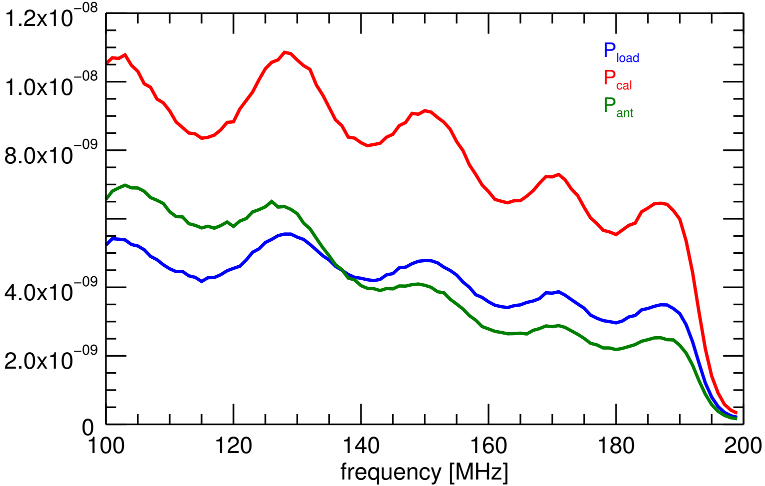

Figure: These spectra were obtained from current EDGES data. Interpolation was used to reduce the frequency resolution to 1 MHz. Some noise remains after interpolation.

Fiducial Values: Antenna and LNA Magnitude

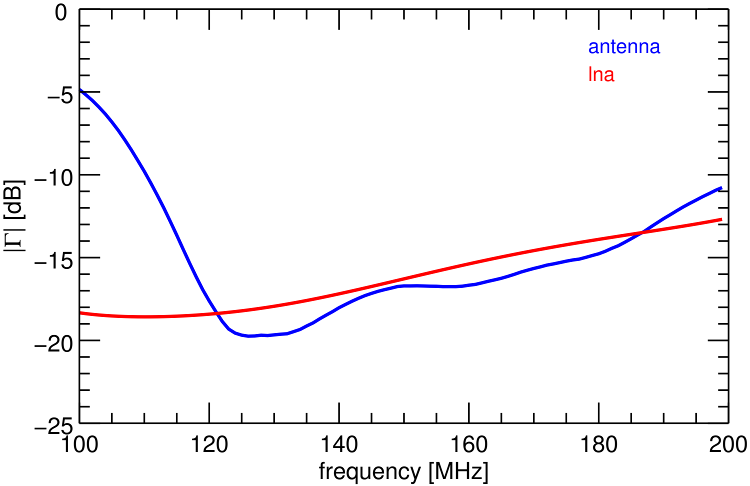

Figure: The reflection of the ferrite-balun antenna is used, expected to be close to the one in the field. It is a measurement performed last year, no interpolation or smoothing involved. The LNA profile was provided by Hamdi. The measurement was very noisy, and therefore modeled using a 5th-order polynomial for smoothing purposes. The red trace is the model.

Fiducial Values: Antenna and LNA Phase

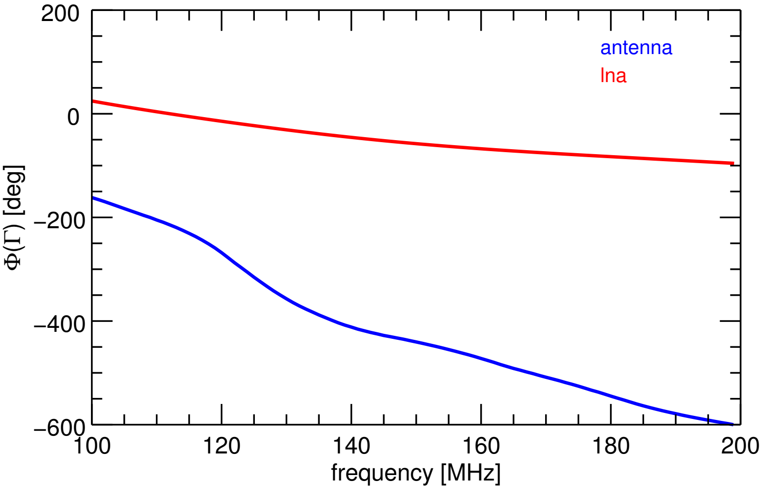

Figure: Same as previous plot.

Description of Method 1

- Vector parameter

$$\bar{\theta} = \left(T_{amb}, T_{cal}, T_c, T_s, T_u, |\Gamma_a|, \phi_a, |\Gamma_l|, \phi_l\right)$$

- Sky temperature

$$T_{sky} = f\left(\bar{\theta}\right) \tag{3}$$

- Error

$$\sigma_{sky}^2 = \sum_{i=1}^{9} \left(\frac{\partial f}{\partial \theta_i}\right)^2 \sigma_{\theta_i}^2 + \sum_{i=1}^{9} \sum_{k \neq i} 2 \frac{\partial f}{\partial \theta_i} \frac{\partial f}{\partial \theta_k} \sigma_{\theta_i \theta_k} \tag{4}$$

Description of Method 1: Matrix Form

$$\sigma_{sky}^2 = \begin{pmatrix} \frac{\partial f}{\partial \theta_1} & \frac{\partial f}{\partial \theta_2} & \cdots & \frac{\partial f}{\partial \theta_9} \end{pmatrix} \begin{pmatrix} \sigma_{\theta_1}^2 & \sigma_{\theta_1\theta_2} & \cdots & \cdots \\ \sigma_{\theta_2\theta_1} & \sigma_{\theta_2}^2 & & \\ \cdots & & & \\ \cdots & & & \sigma_{\theta_9}^2 \end{pmatrix} \begin{pmatrix} \frac{\partial f}{\partial \theta_1} \\ \frac{\partial f}{\partial \theta_2} \\ \cdots \\ \frac{\partial f}{\partial \theta_9} \end{pmatrix}$$

$$\sigma_{sky}^2 = \mathbf{J} \cdot \mathbf{C} \cdot \mathbf{J}^T \tag{5}$$

- The Jacobian matrix **J** is computed symbolically, and then evaluated at the fiducial vector parameter $\bar{\theta}_0$, at each frequency.
- The covariance matrix **C** is generated assuming realistic errors.
- Errors are assigned for one parameter at a time, in order to see their individual impact on the sky temperature.
- No covariance is assigned.

Description of Method 2

In the second method, the propagation of errors is performed as:

$$\Delta T_{sky} = f(\bar{\theta}^{*}) - f(\bar{\theta}_0) \tag{6}$$

- $f(\bar{\theta}) = T_{sky}$
- $\bar{\theta}_0$: fiducial vector parameter
- $\bar{\theta}^{*}$: vector parameter after perturbation of one parameter

Comparison of Methods

The following plots show a comparison of the two methods.

In Method 1, the error in parameter θ_i is characterized by a standard deviation σ_i. The output error is also a standard deviation, always equal or larger than zero.

In Method 2, the input and output are differences with respect to the fiducial values. Since the output difference can be positive or negative, the plots show its absolute value. This simplifies the comparison between the methods.

The assigned errors (or perturbations) are constant in frequency. Two values have been chosen for each parameter, as follows:

- Temperatures: 1 K and 5 K
- Magnitude of reflection coefficient: 0.000115 and 0.00115 (0.01 dB and 0.1 dB at -20 dB)
- Phase of reflection coefficient: 0.1° and 1.0°.

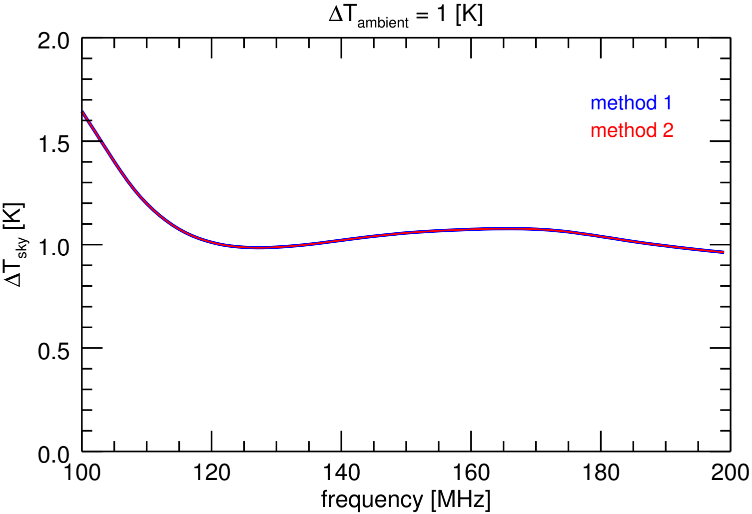

Figure: Results with the two methods overlap.

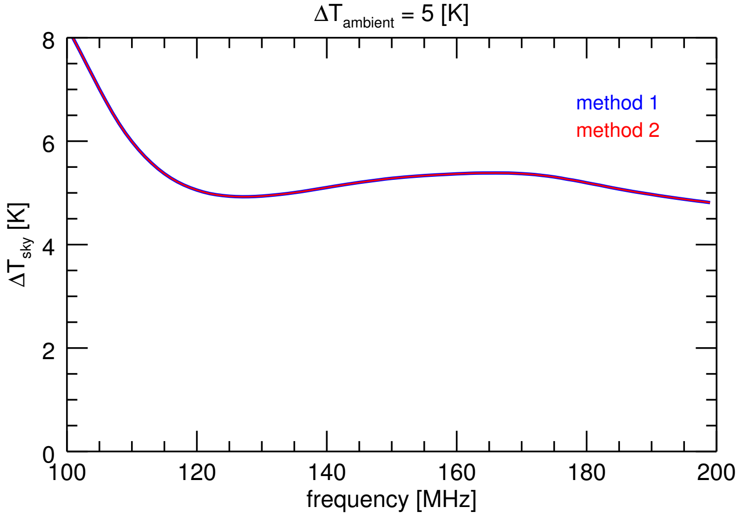

Figure: Results with the two methods overlap.

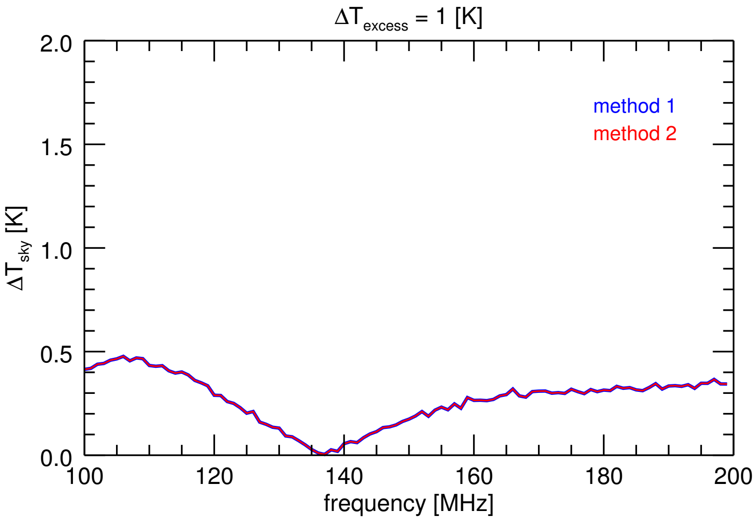

Figure: Results with the two methods overlap. Noise is propagated from that of the spectra (page 7).

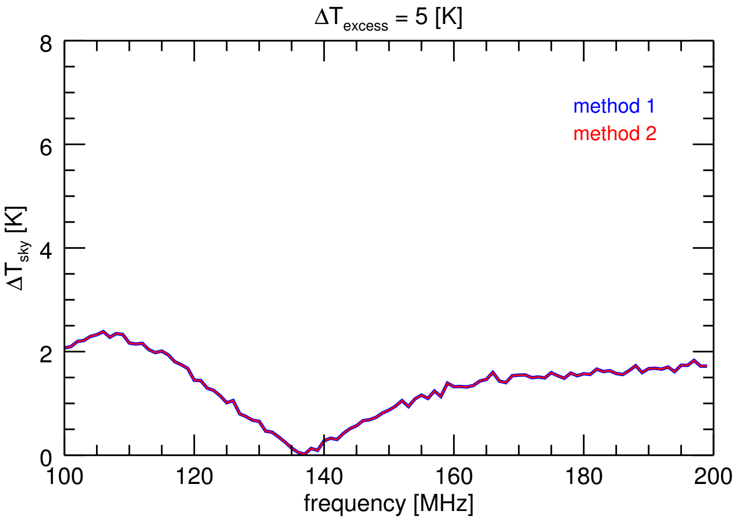

Figure: Results with the two methods overlap. Noise is propagated from that of the spectra (page 7).

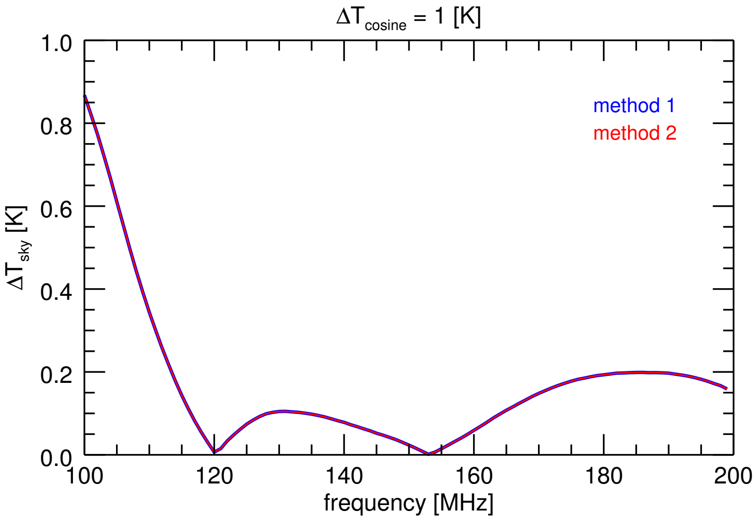

Figure: Results with the two methods overlap.

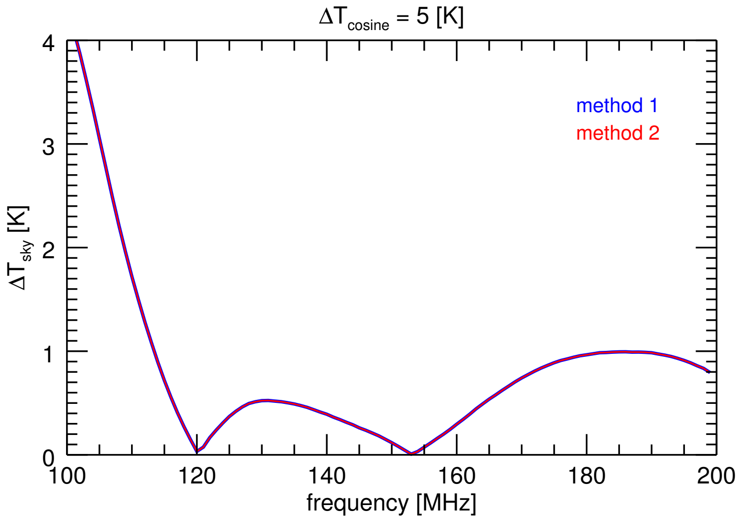

Figure: Results with the two methods overlap.

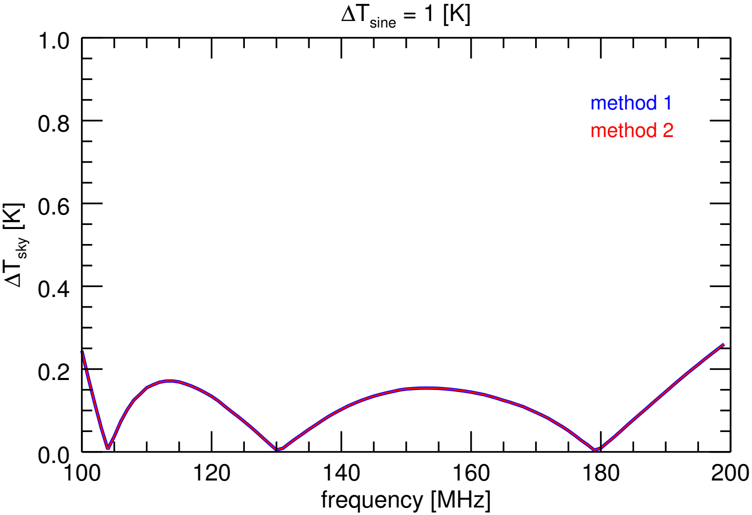

Figure: Results with the two methods overlap.

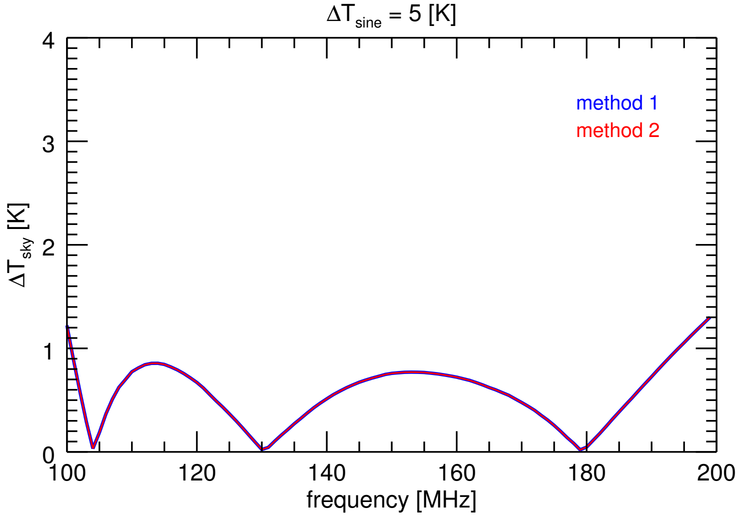

Figure: Results with the two methods overlap.

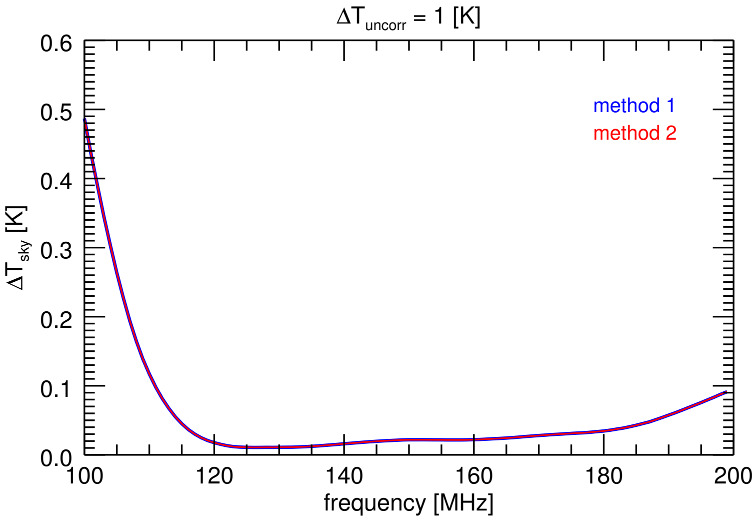

Figure: Results with the two methods overlap.

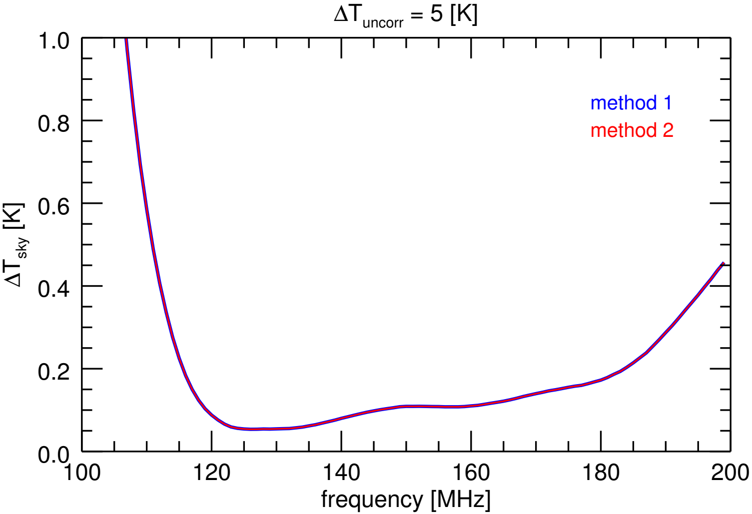

Figure: Results with the two methods overlap.

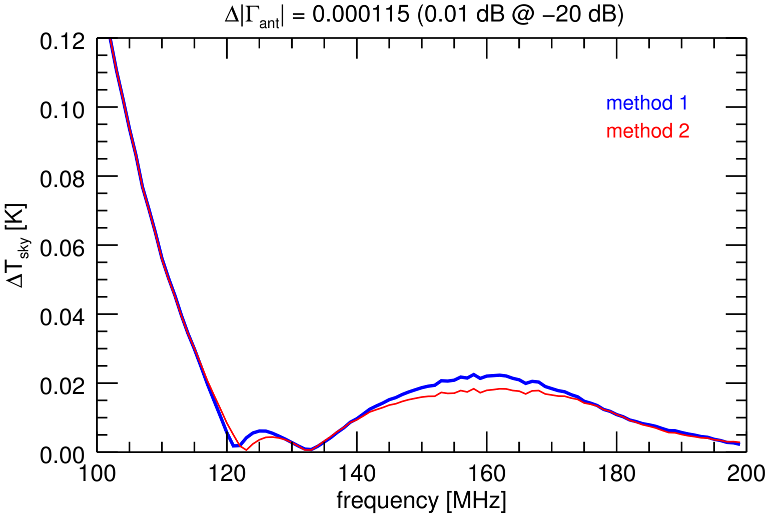

Figure: Differences between methods are evident for the antenna reflection coefficient. They are expected, since equation 1 is non-linear in this parameter. Shape is similar, however, which serves as validation.

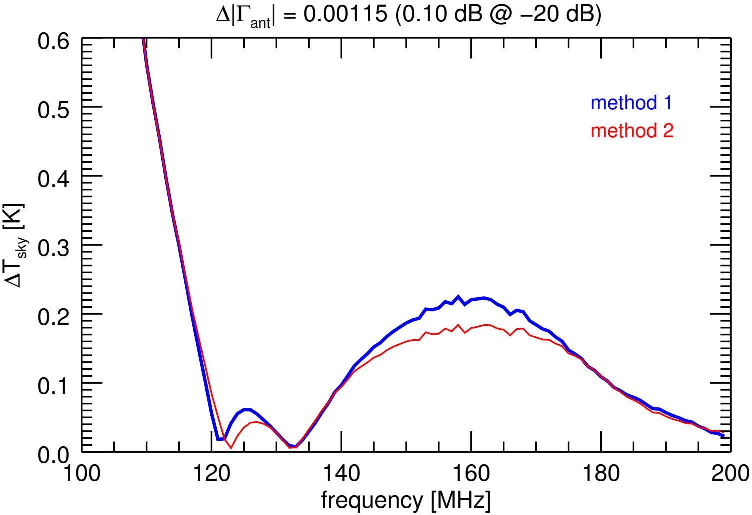

Figure: Differences between methods are evident for the antenna reflection coefficient. They are expected, since equation 1 is non-linear in this parameter. Shape is similar, however, which serves as validation.

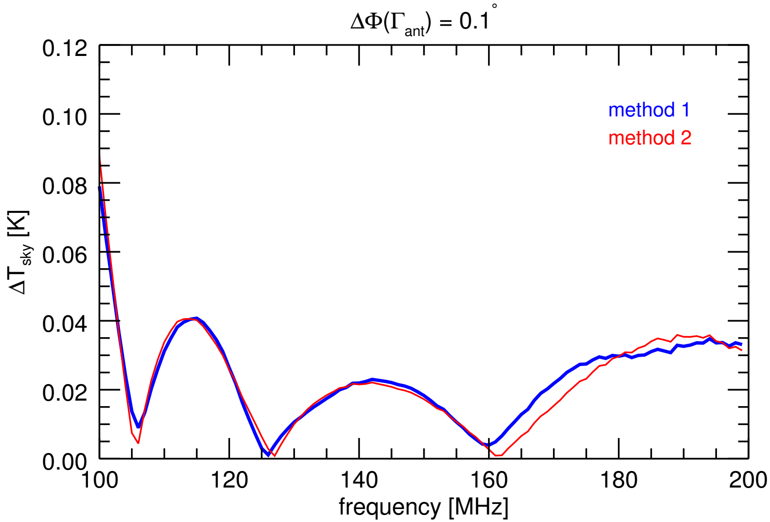

Figure: Differences between methods are evident for the antenna reflection coefficient. They are expected, since equation 1 is non-linear in this parameter. Shape is similar, however, which serves as validation.

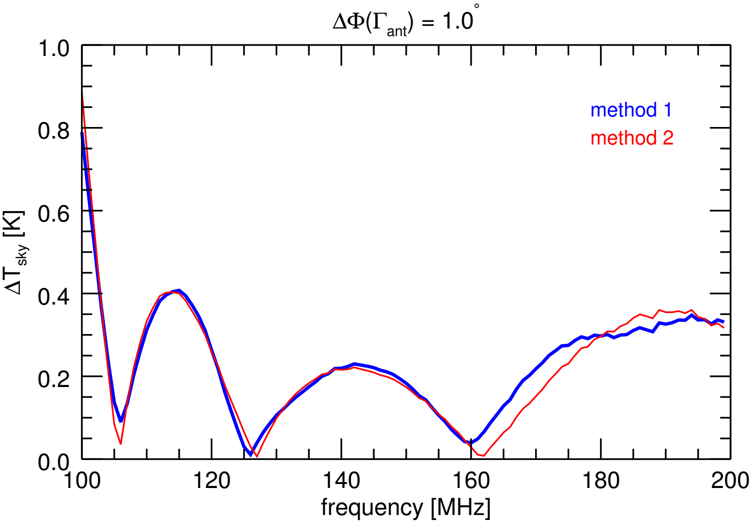

Figure: Differences between methods are evident for the antenna reflection coefficient. They are expected, since equation 1 is non-linear in this parameter. Shape is similar, however, which serves as validation.

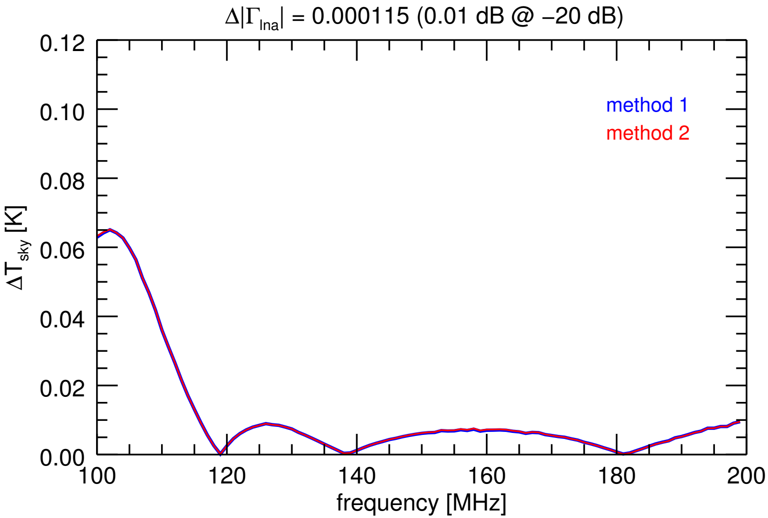

Figure: For the LNA reflection coefficient, the results are almost indistinguishable. At some frequencies the difference seems to increase for larger input error, due to non-linearity.

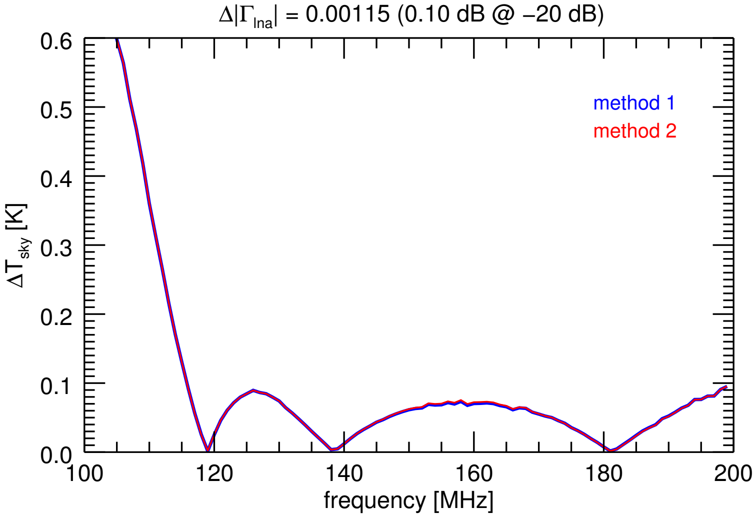

Figure: For the LNA reflection coefficient, the results are almost indistinguishable. At some frequencies the difference seems to increase for larger input error, due to non-linearity.

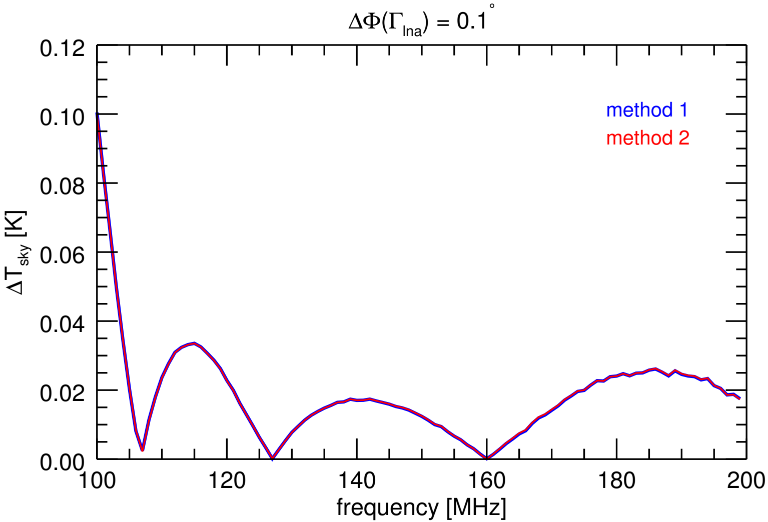

Figure: For the LNA reflection coefficient, the results are almost indistinguishable. At some frequencies the difference seems to increase for larger input error, due to non-linearity.

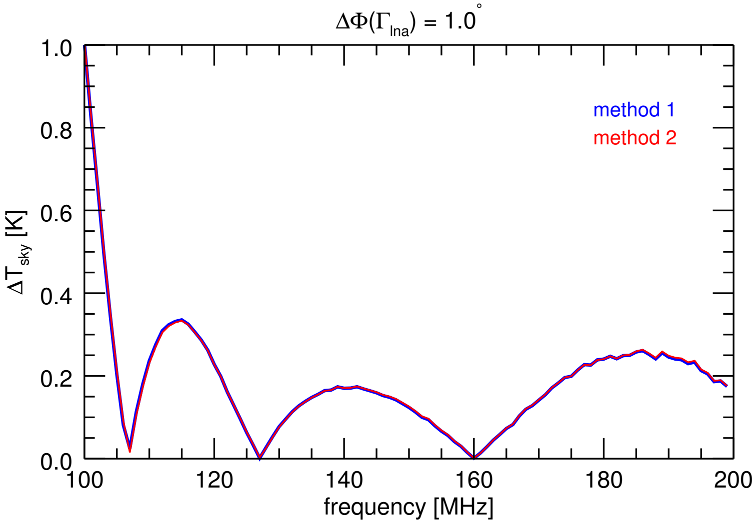

Figure: For the LNA reflection coefficient, the results are almost indistinguishable. At some frequencies the difference seems to increase for larger input error, due to non-linearity.

Summary

The following table summarizes the results, obtained with method 2. This method is preferred since its output error is allowed to be positive or negative.

The RMS value is computed in the range 100-199 MHz, in four ways: 1) direct, 2) after removing an offset, 3) after removing the best-fit function of the form $k \cdot x^{\alpha}$ (k and α are fit parameters), and 4) after removing the best-fit function of the form $k_1 \cdot x^{\alpha} + k_2$ (k_1, k_2, and α are fit parameters).

The results due to errors in reflection coefficients are compared to those presented in Alan's memo 105, for the case with no attenuation between the switch and the LNA (first column of his first table). His results represent the range 50-200 MHz, but this was the closest configuration I found to compare to my results. His results due to temperature errors are not directly comparable to mine, so I do not show them here.

		RMS residuals in mK in 100-199 MHz				
source error	magnitude	direct	offset	scale	scale + offset	Alan's
antenna S_{11}	0.01 dB	36	29	25	22	63
antenna S_{11}	1°	268	259	227	222	417
LNA S_{11}	0.1 dB	201	187	173	140	345
LNA S_{11}	1°	240	237	217	210	398
ambient	1 K	1084	132	106	104	
excess	1 K	295	291	226	73	
cosine	1 K	245	210	202	198	
sine	1 K	127	127	127	127	
uncorrelated	1 K	107	89	82	76	

As the table shows, my results are comparable to Alan's (first four rows). In fact they are always smaller by a factor of 2 approximately. As expected, the errors decrease as more parameters are used to model them. For equal error in temperature, the smallest impact is obtained for the excess and uncorrelated temperatures.

Conclusion

- The impact of instrumental errors on the measured sky temperature has been studied, although for a not-so-realistic instrumental model.
- Two methods of error propagation were used, for purposes of comparison and validation. They provide very similar results for the level of errors assigned to the parameters.
- The nominal (or fiducial) values for some terms of equation 1 had to be interpolated or modeled, in order to use a uniform frequency resolution, and to appreciate the effect of a constant absolute error in the parameters on the sky temperature, with noise remaining sub-dominant.
- The results for the antenna and LNA reflection coefficients are comparable to those presented by Alan in memo 105, although smaller by a factor of 2.
- My analysis is evolving in order to determine the parameter estimation capabilities of EDGES in the presence of sky noise, instrument noise, and foregrounds.